S1270-9638(05)00162-8/FLA AID:2230 Vol.●●●(●●●)
AESCTE:m5+ v 1.50 Prn:18/01/2006; 15:32

aescte2230

[+model] P.1 (1-7)
by:Kris p. 1

Available online at www.sciencedirect.com

SCIENCE DIRECT®

Aerospace Science and Technology ●●● (●●●●) ●●●–●●●

Aerospace Science and Technology

www.elsevier.com/locate/aescte

Control of a decelerating boundary layer. Part 2: Optimization of slotted jets vortex generators

G. Godard [1], J.M. Foucaut, M. Stanislas *

Laboratoire de Mécanique de Lille, France, Bv Paul Langevin, cité Scientifique, 59655 Villeneuve d'Ascq, France

Received 30 September 2005; received in revised form 21 November 2005; accepted 22 November 2005

Abstract

In the first part of this contribution [G. Godard, M. Stanislas, Control of a decelerating boundary layer. Part 1: Optimization of passive vortex generators, Aerospace Sci. Technol., in press], an optimization of passive vortex generators was performed in an adverse pressure gradient boundary layer. The model used was a bump in a boundary layer wind tunnel, which mimics the adverse pressure gradient on the suction side of an airfoil at the verge of separation. The present contribution describes the next step of the study: a test campaign was performed in the same facility to optimize slotted jets devices with both continuous and pulsed blowing. The optimization was done using hot film shear stress probes. The results show quantitatively the improvement brought by the slotted jets devices in terms of skin friction increase. They also show that the tested devices are less effective than equivalent passive devices.

Keywords: Flow control; APG boundary layer; Jets; Vortex generators

1. Introduction

In the first part of this contribution (Godard and Stanislas [1]), a reference passive device configuration was defined in order to compare it to some fluid devices. In fact, passive devices are quite simple to manufacture and it was shown by this study that they can improve significantly the skin friction in an adverse pressure gradient boundary layer, even with a height h/δ of the order of 0.4. The two main problems of such devices are their fragility and the drag increase that they bring permanently. One way to solve both problems would be to make them retractable, using some Micro Electro Mechanical Devices. This is possible at the scale of the thin boundary layer which develops, for example, on the suction side of an extended wing flap. Nevertheless, the involved mechanical complexity and the risk for such systems to be perturbed and even destroyed in the real flight environment have pushed to look more at fluid actuators using air jets. These have the advantage to need only tiny holes in the wall, to be easily cleaned by a strong blowing and to be protected from pollution by a small continuous blowing. On this basis, two main geometries came out: the rectangle and the circle. This paper is devoted to the rectangular configuration. A next paper will focus on round jets. Blowing techniques, first introduced by Taylor [2] in 1947, can use rectangular jets as vortex generators, nevertheless, may be due to manufacturing complexity, this configuration is not very common in the literature. Fig. 1 shows the double slotted jets configuration tested in the present project. As illustrated by Fig. 2, such a device was shown in the previous AEROMEMS project to produces a system of counter rotating quasi streamwise vortices (Bernard et al. [3]). In fact, similar longitudinal vortices, resulting from the complex interaction of a single rectangular jet with a cross flow, have been observed in both experimental (Zhang [4–7]) and numerical studies (Akanni and Henry [8]). These vortices are quite similar to those produced by passive vane-type vortex generators (Zhang [5]; Bernard et al. [3]). In the AEROMEMS project, good results were obtained with pulsed jets with a high velocity amplitude. These results were fairly insensitive to the frequency of the jet pulsation. It is important to notice that no lift-off was observed in the counter rotating configu-

* Corresponding author. Tel.: +33 03 20 33 71 70; fax: +33 03 20 33 71 69.
E-mail address: stanislas@ec-lille.fr (M. Stanislas).
[1] Presently: CORIA, UMR CNRS 6614, Rouen, France.

1270-9638/$ – see front matter
doi:10.1016/j.ast.2005.11.006

Nomenclature

Latin symbols

C_d	drag coefficient	
C_f	skin friction coefficient, $C_f = \frac{\tau_p}{\frac{1}{2}\rho U_e^2}$	
Cq_δ	total flow coefficient	
dP/dx	pressure gradient	Pa/m
e	width of the slots	mm
H	height of the bump	m
H_{12}	shape factor, $H_{12} = \frac{\delta^*}{\theta}$	
H_{32}	shape factor, $H_{32} = \frac{\delta^{**}}{\theta}$	
l	length of the slots	mm
L	transverse separation between two slots in the CtR configuration	mm
U, V	velocity components tangential and normal to the surface	m/s
U_e	external velocity	m/s
U_{inf}, U_∞	freestream velocity	m/s
u_τ	friction velocity	m/s
x, y, z	longitudinal, vertical and transverse coordinates	m
X_d	abscissa of the devices	m

Greek symbols

β	skew angle of the slots	°
δ	boundary layer thickness	m
δ^*	displacement thickness	m
θ	momentum thickness	m
δ^{**}	energy thickness	m
η	coordinate normal to the bump	m
η^+	dimensionless coordinate normal to the bump, $\eta^+ = \frac{\gamma U_\tau}{v}$	
λ	distance between two devices	m
λ^+	dimensionless distance between two devices, $\lambda^+ = \frac{\lambda U_\tau}{v}$	
τ	wall shear stress with actuation	kg/m^2 s
τ_0	wall shear stress without actuation	kg/m^2 s
$\Delta\tau$	$\tau - \tau_0$	kg/m^2 s
ΔP	pressure difference	Pa
Δz	lateral displacement	m
ΔX_{vg}	streamwise distance between the vortex generators line and the minimum skin friction station	

Abbreviations

BL	boundary layer
ZPGBL	zero pressure gradient boundary layer
APGBL	adverse pressure gradient boundary layer
CoR	co-rotating
CtR	counter-rotating
VG	vortex generator

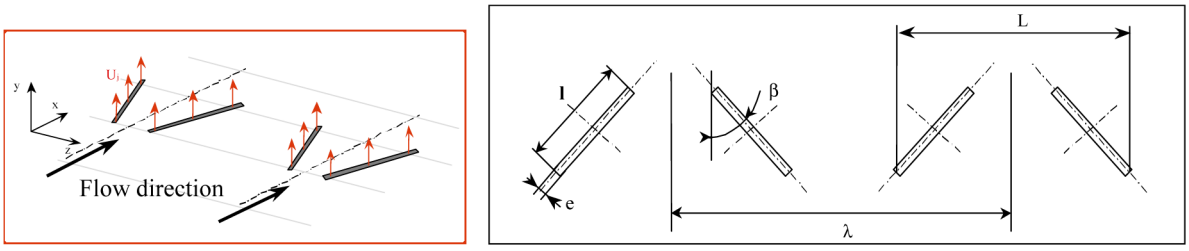

Fig. 1. (a) Counter rotating slot device configuration, (b) geometrical parameters.

Table 1
Effective parameters used in previous slotted jets vortex generators studies

	Model used	Configuration	α (°)	β (°)	e/l	Φ_h/δ	λ/L	VR_e
Zhang 1997–2000	ZPGBL	Single steady jet	30	15	1/5	0.58	–	1
Bernard 2000	APGBL (Bump)	CtR double slot pulsed jet	0	45	1/30	0.019	5.17	5

ration (Bernard et al. [3]), while a strong penetration through the boundary layer (reducing the control effectiveness) was observed for a single rectangular jet in zero pressure gradient BL by Zhang [4]. It is important to notice too that, in the literature (Zhang [4–7]; Akanni and Henry [8]; Vronski [9]), the rectangular jet is pitched and skewed. The best parameter choice for turbulent boundary layer control obtained by Zhang [4–7] is compared in Table 1 with the parameters of Bernard et al. [3] in the AEROMEMS study. α is the pitch angle, β the skew angle, e the slot thickness, l the slot length, Φ_h the hydraulic diameter, δ the boundary layer thickness, λ the transverse devices spacing, L the distance between two slots of the same device and VR_e the ratio of the jet velocity to the BL external velocity. As seen from this table, there are significant differences between the respective velocity ratios used in both studies. It was thus of interest to vary the parameters of the present configuration, in order to optimize it and compare it quantitatively with the passive devices characterized in Godard and Stanislas [1].

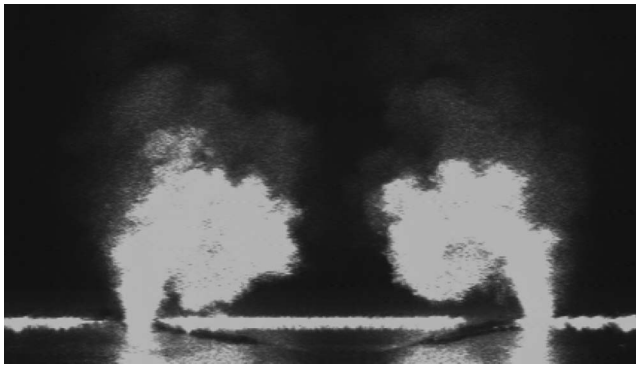

Fig. 2. Light sheet/smoke visualization of the counter-rotating vortices generated by a system of two slots as in Fig. 1 (a). The light sheet is normal to the wall and to the flow, just downstream of the actuators. From Bernard et al. [2].

2. Experimental set-up

The experimental set-up is a bump on the lower floor of a boundary layer wind tunnel which mimics the flow on the suction side of an airfoil at high angle of attack (but without separation). It will not be detailed here, as it is the same as the one used by Godard and Stanislas [1] and by Bernard et al. [3, 10]. Only the specific actuators will be described.

Fig. 1 gives the geometry and Fig. 3 shows a photograph of the devices which were manufactured. Each actuator is composed of two slots of width e and length l. These two slots are symmetric and form an angle β with the streamwise x axis.

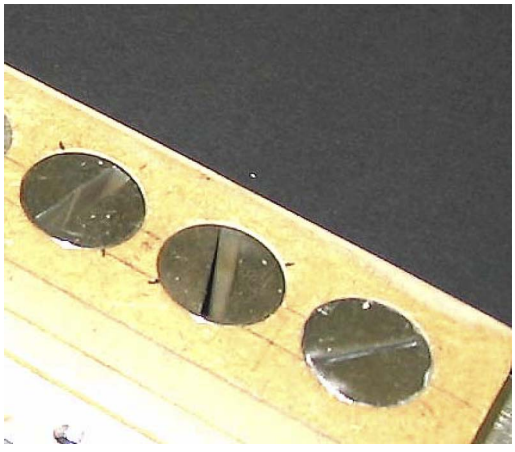

Fig. 3. Slotted jets device used for the parametric study.

They are separated by a distance L which follows the definition used for the passive devices by Godard and Stanislas [1] and which thus depends on β as the slots rotate around a point located at their mid length. The spanwise spacing between two actuators is λ. These actuators were settled in a rectangular opening located in the middle of the wind tunnel at $X_d = 17.55$ m. A rectangular cap was manufactured with a series of cylindrical holes at a constant spacing of 20 mm. This cap was made of a thick wooden plate glued on a thin aluminum plate. In each cylindrical hole, a steel cap containing a rectangular nozzle could be fitted. The nozzles were manufactured by electro-erosion, in order to obtain an accurate slot size and a smooth nozzle shape. Different series of steel caps were manufactured with different slot width ($e = 0.5, 1, 2, 3$ mm). The slot length was fixed at 15 mm. With such a device, the spacing and skew angle of the slots were easily varied. The whole row of slots was fed from the backside, either from a settling chamber for continuous blowing or from a loudspeaker system for pulsating jets.

All the measurements were performed using the hot film shear stress probes described in Godard and Stanislas [1].

The flow without control was also the same as in Godard and Stanislas [1] and as previously characterized in detail by Bernard et al. [10].

3. Optimization results

3.1. Test description

Fig. 1 gives the geometrical characteristic parameters of the double slot device. As compared to the passive device, the only new parameter is the slot thickness e. At the actuators location, the boundary layer thickness is $\delta = 16.5$ cm. Table 2 gives the parameters which were varied and the range of values tested in the study. Φ_h/δ is the ratio of the jets hydraulic diameter to the boundary layer thickness, VR_e is the ratio between the jet velocity and the local free stream velocity, f_p is the frequency of pulsation of the jets. As explained in Section 2, cylindrical steel knobs, containing one slot, are plugged in a plate with the corresponding hole. The knobs can be easily turned to adjust the skew angle β, while changing the plate allows to vary the spacing λ. The aspect ratio e/l was varied by manufacturing different knobs. The test procedure was the same as for the optimization of the passive systems. For each variation of

Table 2
Range of values of double slot jet device parameters tested

Model used	VGJ	α (°)	β (°)	e/l	Φ_h/δ	λ/L	VR_e	f_p (Hz)
APGBL (Bump)	CtR slots		15	1/30	0.019	1.66	1.17	80
		0	–	–	–	–	–	–
			45	3/15	0.046	7	6.65	180

Table 3
Counter-rotating slots, optimal configuration

VR	e/l	L/δ	L/l	λ/l	β (°)	$\Delta\tau/\tau$ (%)
6	1/15	0.099	2.08	6.87	15	70/55

the geometry, a jet velocity range between 10 m/s and 80 m/s ($1.17 < \mathrm{VR_e} < 6.65$) was investigated. Note should be taken of the fact that the pitch angle was held constant ($\alpha = 0°$) because, in contradiction to the literature (Zhang [5]), no vortex lift-off was observed in the previous AEROMEMS study. The first part of the optimization procedure was applied to the continuous jets configuration. The effect of the pulsation of the jets was tested only for the best continuous configuration. Table 3 gives the starting parameters for this optimization study.

3.2. Results

3.2.1. Continuous blowing

The active devices tests results are presented with the same normalization as for the passive devices in Godard and Stanislas [1]. The starting configuration was close to the AEROMEMS study by Bernard et al. [3]. The devices are located at the same streamwise position along the bump ($X_\mathrm{d} = 17.55$ m). Three counter rotating systems (1 system = 2 slots) are located symmetrically with respect to the wind tunnel vertical central plane. Skin friction measurements were performed at the same streamwise location as for the passive devices ($X_{\mathrm{Cfmin}} = 18.58$ m). In the spanwise direction, the probes are on the counter-rotating system axis ($z/\lambda = 0$) and halfway between two systems ($z/\lambda = 0.5$).

Figs. 4, 5 and 6 show the effect of the skew angle (β), slot spacing (L/l) and jet velocity ratio $\mathrm{VR_e}$ on the skin friction. Fig. 4 shows positive $\Delta\tau/\tau_0$ values for $\mathrm{VR_e} \approx 3$. The $\Delta\tau/\tau_0$ difference in the spanwise direction increases with decreasing β. For $\beta = 15°$ and $\mathrm{VR_e} = 6$, the $\Delta\tau/\tau_0$ difference reaches 30%. $\Delta\tau/\tau_0$ is more sensitive to β between two devices ($z/\lambda = 0.5$) than on the axis ($z/\lambda = 0$).

Fig. 5 shows positive $\Delta\tau/\tau_0$ values from $\mathrm{VR_e} \approx 2$. The $\Delta\tau/\tau_0$ slope is lower than in Figs. 4 and 6. The curve tend to level off just before $\mathrm{VR_e} = 4$ and sharply increase from $\mathrm{VR_e} = 5$. From $\mathrm{VR_e} = 2$ up to 3.5, $\Delta\tau/\tau_0$ is a bit higher than with $L/l = 1.37$. For $\mathrm{VR_e} > 3.5$ it is lower. The spanwise distribution seems to be a function of $\mathrm{VR_e}$, whatever β is. Higher $\Delta\tau/\tau_0$ values (+65%) are found at both spanwise position for $\beta = 25°$ with $\mathrm{VR_e} = 6$.

In Fig. 6 $\Delta\tau/\tau_0$ is sensitive to β. The limit of efficiency ($\mathrm{VR_e} \approx 2$) is found for the lowest skew angle ($\beta = 15°$). There is no significant $\Delta\tau/\tau_0$ difference in spanwise direction. In the best case ($\beta = 15°$), from $\mathrm{VR_e} = 2$ up to $4.25\Delta\tau/\tau_0$ is higher than in Fig. 4 ($L/l = 1.37$). For $\mathrm{VR_e} > 4.25$ it is slightly lower.

In spite of its higher limit of efficiency ($\mathrm{VR_e} = 3$) and a significant $\Delta\tau/\tau_0$ spanwise variation, Fig. 4 shows results which are the less sensitive to β. This aspect is important in terms of robustness for an aircraft device. This configuration preserves maximum skin friction variations from $\mathrm{VR_e} = 4$ up to $\mathrm{VR_e} = 6.5$ at halfway, with a highest value of 100% for $\mathrm{VR_e} = 6$ and $\beta = 15°$. These values of β and L/l were chosen for the following tests.

Fig. 7 shows the effect of the system spacing (λ/l) and jet velocity ratio $\mathrm{VR_e}$ on the skin friction. For $\lambda/l = 4.12$, the results are much poorer than for the other values. This may be attributed to a lift-off phenomena. On the system axis, the re-

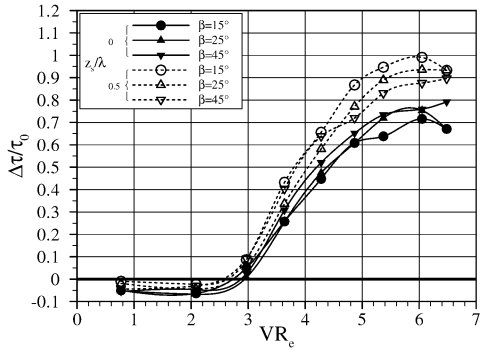

β (°)	15 - 45
e/l	1/15
L/l	**1.37**
λ/l	6.87
VR_e	0.75-6.7
F_p(Hz)	0

Fig. 4. Skin friction increase as a function of jet velocity for different skew angles and $L/l = 1.37$.

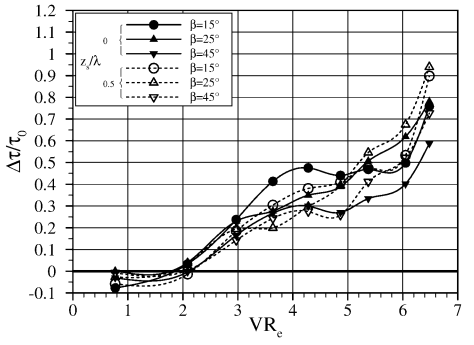

β (°)	15 - 45
e/l	1/15
L/l	**2.75**
λ/l	6.87
VR_e	0.75-6.7
F_p(Hz)	0

Fig. 5. Skin friction increase as a function of jet velocity for different skew angles and $L/l = 2.75$.

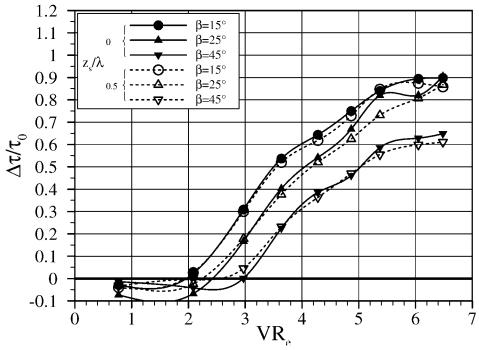

β (°)	15 - 45
e/l	1/15
L/l	**4.12**
λ/l	6.87
VR_e	0.75-6.7
F_p(Hz)	0

Fig. 6. Skin friction increase as a function of jet velocity for different skew angles and $L/l = 4.12$.

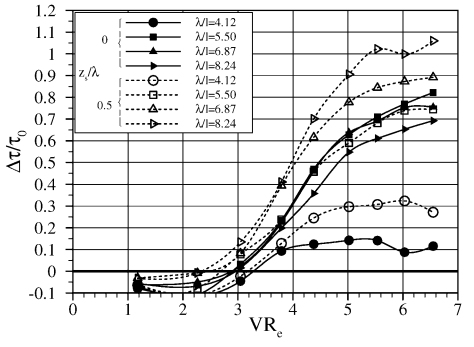

β (°)	15
e/l	1/15
L/l	1.37
λ/l	4.12-8.24
VR_e	1.18-6.55
F_p(Hz)	0

Fig. 7. Skin friction increase as a function of jet velocity for different distances between two systems.

sults are fairly close for the three higher values of λ/l, although a visible decrease is observed at $\lambda/l = 8.24$. The sensitivity to this parameter is clearly important at $z/\lambda = 0.5$, where $\Delta\tau$ increases regularly with λ/l in the studied range. Consequently the spanwise variation increases also. Looking at the results, it can be expected that by increasing again λ/l, the values at $z/\lambda = 0.5$ will at least level off, while the values at $z = 0$ will further decrease. Consequently, a value of $\lambda/l = 6.87$ was retained as a best compromise for the following tests.

Fig. 8 shows the effect of the slots aspect ratio for the chosen range of VR_e. For the largest slots, air compressor constraint have limited the maximum jet velocity to $VR_e = 3.91$. Nevertheless, Fig. 8 shows a significant reduction of the limit of efficiency when e/l increases (VR_e limit $= 2.8$; 1.5 and 0.80 for $e/l = 1/15$; 2/15 and 3/15 respectively). The VR_e necessary to produce the best results ($\Delta\tau/\tau_0 \approx 100\%$) is also reduced ($VR_e = 6$; 4.8; 4.2 for $e/l = 1/15$; 2/15 and 3/15 respectively). Fig. 9 shows the effect of the flow rate coefficient Cq_δ on $\Delta\tau/\tau_0$. This coefficient is defined as:

$$Cq_\delta = \frac{\rho_j V_j A_j}{\rho_e V_e \delta\lambda}$$

where ρ_j, V_j, and A_j are respectively the jet density, velocity and cross-section, ρ_e V_e, δ and λ are the density and velocity outside the BL at the station of the jet, δ the boundary layer thickness and λ the spacing between two devices.

Of interest is the fact that all curves have approximately the same origin in this representation, indicating that a minimum flow rate is needed to obtain a significant effect. The second point is that the slope at the origin is decreasing when e/l increases. On the contrary, the maximum value reached seems to be more or less constant, but it is reached for increasing values of Cq_δ. Figs. 8 and 9 show that to reach a given value of $\Delta\tau/\tau_0$, increasing the slot thickness (e) allows to decrease VR_e, but at the expense of increasing Cq_δ. For example at $Z_s/\lambda = 0.5$, a $\Delta\tau/\tau_0 = 60\%$ requires a 32% reduction of VR_e and a 40% increase of Cq_δ when the slot thickness is doubled from $e/l = 1/15$ to $e/l = 2/15$.

Table 3 gives the best set of parameters found for this actuators configuration and the corresponding improvement in skin friction. These values can be directly compared to the results obtained with passive devices by Godard et al. [1]. Obviously the slotted jets are much less effective than the passive devices (by a factor of about 2).

3.2.2. Pulsed blowing

In the first AEROMEMS project (Bernard et al. [3]), pulsating jets were developed and studied extensively. In the slotted configuration under study, the conclusion was that the jet pulsation was not changing fundamentally the physics of the actuating flow. It was mainly allowing to save half of the flow rate by using a sinusoidal jet velocity with a maximum value comparable to that of an equivalent continuous blowing. This result was independent on the frequency in the range 50–150 Hz.

It was of course of interest to check the pulsation effect in the present optimal configuration, which is fairly different from the initial one (see Tables 2 and 3). For that purpose, the same method was used: the whole array of devices was fed by a rectangular pipe with a 2×20 cm^2 cross section. Two loud speakers of 20 cm in diameter were fitted in the two walls of the channel (face to face). The moving cone was filled with foam to keep the pipe rectangular in cross section. The two loud speakers were driven by a stereo amplifier and the input signal was provided by a PC computer. The channel was fed, from the bottom, by a settling chamber. This allowed to apply the pulsation on a non-zero mean velocity. The system could be operated up to 200 Hz, with outlet velocities up to 70 m/s.

Figs. 10 and 11 show the instantaneous jets velocity obtained in respectively a suction/blowing pulse cycle (no mean flow rate) and a purely blowing pulsed cycle, measured with a single hot wire anemometer.

In Fig. 10, the higher peak is due to the blowing and the lower peak is due to the suction phase (rectification of the negative velocities by the HWA). The suction phase can be eliminated by adding a continuous air flow in the system (Fig. 11). Two different frequencies (80–180 Hz) were tested in this study, in the range allowed by the pulsating device. Different mean velocity profiles of the jets were measured at five positions along a slot, to confirm the jet homogeneity which was very good. Figs. 12 and 13 show the pulsed jets effect on the skin friction variation. Each figure includes results of continuous jets, blowing/suction pulsed jets and blowing only pulsed jets. In all cases the blowing/suction configuration gives the worst results. The continuous jets give better results than the pulsed jets at $F_p = 80$ Hz. At $F_p = 180$ Hz, the blowing pulsed jets are

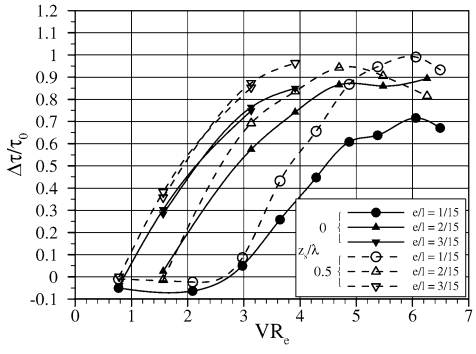

β (°)	15
e/l	*1/15 - 3/15*
L/l	1.37
λ/l	6.87
VR$_e$	*0.78-6.5*
F$_p$(Hz)	0

Fig. 8. Skin friction increase as a function of jet velocity for different slots thicknesses.

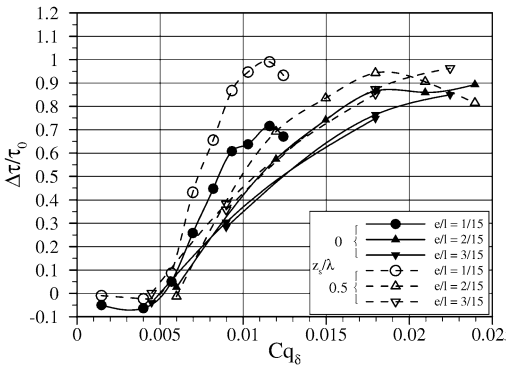

β (°)	15
e/l	1/15 - 3/15
L/l	1.37
λ/l	6.87
VR$_e$	0.78-6.5
F$_p$(Hz)	0

Fig. 9. Skin friction increase as a function of Cq_δ for different slots thickness.

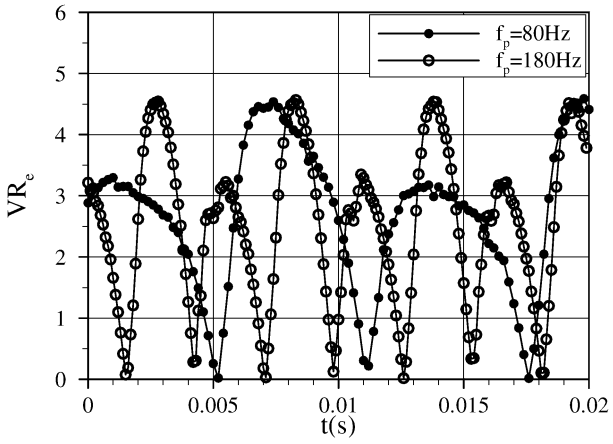

Fig. 10. Hot wire velocity signals of blowing/suction pulsating jet.

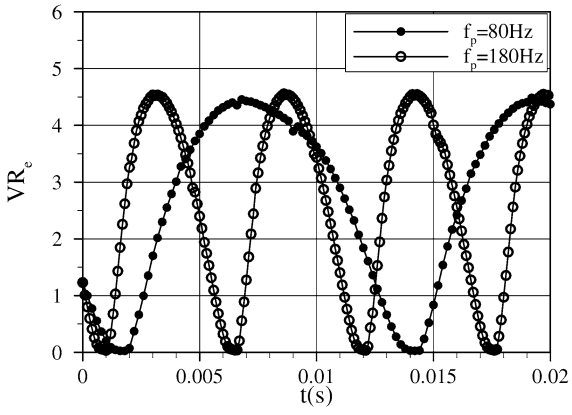

Fig. 11. Hot wire velocity signals of blowing pulsating jet.

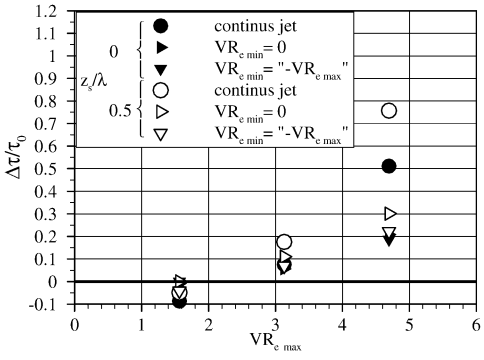

β (°)	15
e/l	1/15
L/l	1.37
λ/l	6.87
VR_emax	***1.56 3.13 4.69***
f_p(Hz)	**80**

Fig. 12. Skin friction increase as a function of jet velocity for different pulsating configurations ($f_\mathrm{p} = 80$ Hz).

slightly better than the continuous ones for $\mathrm{VR_e} \leqslant 3$. Both are comparable at $\mathrm{VR_e} = 4.7$. As the tests performed by Bernard et al. [2] did correspond to high jet velocities and for blowing only jets, the present results confirm the conclusions of this preliminary study.

4. Conclusion

An experiment was performed to test and optimize counter-rotating slotted jet actuators in order to control a decelerating boundary layer. Several parameters of the device were varied

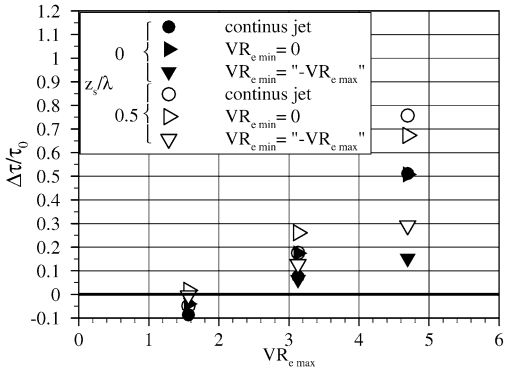

β (°)	15
e/l	1/15
L/l	1.37
λ/l	6.87
VR_emax	***1.56 3.13 4.69***
f_p(Hz)	**180**

Fig. 13. Skin friction increase as a function of jet velocity for different pulsating configurations ($f_\mathrm{p} = 180$ Hz).

and their influence on the skin friction variation along the wall was assessed. The influence of the tested parameters can be summarized as follows:

- Velocity ratio ($\mathrm{VR_e}$)
  The performances increase with increasing $\mathrm{VR_e}$.
- Skew angle (β)
  The results show a skew angle sensitivity. The skin friction increases with β decreasing. The best value tested is around 15°. Zhang [6] found the same value, which it is close to the best value found by Godard et al. [1] for passive devices.
- Slots spacing (L/l)
  An optimum slots spacing does not appear. It must be recalled that in the present experiment, the slots spacing varies slightly when β is changed. The effect of this parameter is evidenced in Figs. 4 to 6. For small values of L/l, the efficiency is good and the sensitivity to β is low. For intermediate values of L/l, an improvement is observed at low velocity ratios but the efficiency decreases for higher $\mathrm{VR_e}$. For large values of L/l, the efficiency is improved for all $\mathrm{VR_e}$, but a significant sensitivity to β is observed, together with a better transverse homogeneity.
- System spacing (λ/l)
  The results show the importance of this parameter. For low values, the results seem to indicate an ejection of the vortices away from the wall. This leads to a high spanwise variation of the skin friction. In the present tests, the value of $\lambda/l = 6.87$ gives the higher shear stress improvement for $\mathrm{VR_e} = 6$.
- Slot thickness (e/l)
  An increase of the slot thickness results in shifting the $\Delta\tau/\tau_0$ curve toward lower $\mathrm{VR_e}$. This results in a significant reduction of the minimum usable value of $\mathrm{VR_e}$. However for a given value of $\Delta\tau/\tau_0$, Cq_δ increases with increasing the slot thickness. This result is in good agreement with Zhang [4,6] studies, who used $e/l \sim 3/15$ with $\Phi_\mathrm{h}/\delta = 0.056$, in our case $\Phi_\mathrm{h}/\delta = 0.046$.
- Pulsation frequency f_p
  The results show that pulsating the jets without suction produces a higher efficiency for $f_\mathrm{p} = 180$ Hz than for 80 Hz. For $\mathrm{VR_{e\,max}} < 3.5$, the results are slightly better at 180 Hz than with the steady jet. They are comparable for

$VR_{e\,max} = 4.70$. At the lower frequency ($f_p = 80$ Hz) the results are not good.
Whatever the pulsed frequency is, the blowing/suction (synthetic jet) configuration shows a very low effectiveness as compared to the steady jet configuration.

Finally, it must be mentioned that for a geometrical configuration roughly comparable to the passive devices in term of – skew angle (β) – system and – slots spacing, the wall shear stress evolution in the spanwise direction shows significant differences. The maximum skin friction variation with respect to the smooth wall is located here between two devices. This characteristic differs from that of counter rotating passive VGs which evidence this maximum around the plane of symmetry of each device. This would suggest a change of sign of the vortices between the two configurations. This point was not investigated further as the effectiveness of the slotted jets actuators appeared not so good. It was decided at this stage to characterize round jets actuators. It should be indicated that the tilt angle of the jets was not investigated in the present study although other authors seem to obtain better results with tilted slotted jets (Zhang [4–7]).

Acknowledgements

The research reported here was undertaken as part of the AEROMEMS II project (Advanced Aerodynamic Flow Control Using MEMS, Contract No G4RD-CT-2002-00748). The AEROMEMS II project is a collaboration between BAE SYSTEMS, Dassault, Airbus Deutschland GmbH, EADS-Military, Snecma, ONERA, DLR, LPMO, Manchester University, LML, Warwick University, TUB, Cranfield University, NTUA, and Auxitrol. The project is funded by the European Union and the project partners.

References

[1] G. Godard, M. Stanislas, Control of a decelerating boundary layer. Part 1: Optimization of passive vortex generators, Aerospace Sci. Technol., in press.
[2] H.D. Taylor, The elimination of diffuser separation by vortex generators, United Aircraft Corporation Report No R-4012-3, June 1947.
[3] A. Bernard, P. Dupont, J.M. Foucaut, M. Stanislas, Identification and assessment of flow actuation and control strategies, AEROMEMS report FREP/CN18/MS001101, 2000.
[4] X. Zhang, H.-L. Zhang, M.W. Collins, Some aspects of streamwise vortex production using air jets, AIAA paper 96-020, 1996.
[5] X. Zhang, M.W. Collins, Measurements of a longitudinal vortex generated by a rectangular jet in a turbulent boundary layer, Phys. Fluids 9 (6) (1997) 1665–1673.
[6] X. Zhang, An inclined rectangular jet in a turbulent boundary layer-vortex flow, in: Experiments in Fluids, vol. 28, 2000, pp. 344–354.
[7] X. Zhang, Turbulence measurements of an inclined rectangular jet embedded in a turbulent boundary layer, Internat. J. Heat Fluid Flow 21 (2000) 291–296.
[8] S.D. Akanni, F.S. Henry, Numerical calculations for air jet vortex generators in turbulent boundary layer, in: CEAS European Forum on High Lift & Separation Control, March, 1995, Bath, UK.
[9] T. Vronski, High performance cost-effective large wind turbine blades using air jet vortex generators, ETSU report no W/41/00541, http://www.dti.gov.uk/energy/renewables/publications/pdfsAV4100541.pdf, 2000.
[10] A. Bernard, P. Dupont, J.M. Foucaut, M. Stanislas, Decelerating boundary layer: a new scaling and mixing length model, AIAA J. 41 (2) (2003) 248–255.